Effects of molecular rotation after ionization and prior to fragmentation on observed recoil-frame photoelectron angular distributions in the dissociative photoionization of nonlinear molecules

Jesús A. López-Domínguez and Robert R. Lucchese

Phys. Rev. A **93**, 033421 — Published 31 March 2016

DOI: 10.1103/PhysRevA.93.033421

Effects of molecular rotation after ionization and prior to fragmentation on observed recoil-frame photoelectron angular distributions in the dissociative photoionization of non-linear molecules

Jesús A. López-Domínguez and Robert R. Lucchese*

Department of Chemistry,

Texas A&M University,

College Station, Texas 77843-3255

Abstract

Experimental angle-resolved photoelectron-photoion coincidence experiments measure photoelectron angular distributions (PADs) in dissociative photoionization (DPI) in the reference frame provided by the momenta of the emitted heavy fragments. By extension of the nomenclature used with DPI of diatomic molecules, we will refer to such a PAD as a recoil-frame PAD (RFPAD). When the dissociation is fast compared to molecular rotational and bending motions, the emission directions of the heavy fragments can be used to determine the orientation of the the bonds that are broken in the DPI at the time of the ionization, which is known as the axial-recoil approximation (ARA). When the ARA is valid, the RFPADs correspond to molecular-frame photoelectron angular distributions (MFPADs) when the momenta of a sufficient number of the heavy fragments are determined. When only two fragments are formed, the experiment cannot measure the orientation of the fragments about the recoil axes so that the resulting measured PAD is an azimuthally-averaged RFPAD (AA-RFPAD). In this study we consider how the breakdown of the ARA due to rotation will modify the observed RFPADs for DPI processes in non-linear molecules for ionization by light of arbitrary polarization. This model is applied to the core C $1s$ DPI of CH_4 with the results compared to experimental measurements and previous theoretical calculations done within the ARA. The published results indicate that there is a breakdown in the ARA for two-fragment events where the heavy fragment kinetic energy release (KER) was less than 9 eV. Including the breakdown of the ARA due to rotation in our calculations gives very good agreement with the experimental AA-RFPAD leading to an estimate of upper bounds on the predissociative lifetimes as a function of the KER of the intermediate ion states formed in the DPI process.

Keywords: Rotational motion, molecular photoionization, non-linear molecules, MFPAD, RFPAD

* lucchese@mail.chem.tamu.edu

I. INTRODUCTION

Obtaining information on the dynamics of photodissociation processes can be accomplished experimentally by measuring the photo-fragment emission direction using linearly polarized light [1]. It has been observed that the photofragment angular distribution can be peaked parallel or perpendicular to the incident light beam [2]. For a one-photon photodissociation of an unpolarized sample within the dipole approximation, the normalized photofragment angular distribution is given by [3, 4],

$$I(\theta) = \frac{1}{4\pi}\left[1 + \beta P_2(\cos\theta)\right] \tag{1}$$

where θ is the angle between the recoil direction and the direction of polarization of the light, and $P_2(\cos\theta)$ is the second-order Legendre polynomial. The anisotropy parameter β depends on the orientation in the molecular framework of the transition dipole moment, the dissociation direction and on the vibrational and rotational dynamics of the photo-excited molecules, as shown by Bersohn [3, 5], Jonah [6] and others. When the molecule dissociates rapidly after the absorption of light and the kinetic energy of dissociation is large compared to the kinetic energy of rotation, corresponding to the axial-recoil approximation (ARA), the parameter β takes the simple form $\beta = 2P_2(\cos\chi)$, where χ is the angle between the transition moment and the direction of dissociation, *i.e.* in the recoil direction [3]. The β parameter values can range from +2 to -1 for a pure parallel transition and a pure perpendicular transition respectively when assuming the ARA. If the molecule is rotating, there are different possible effects, one, when the dissociation is not instantaneous, leading to a metastable excited state of the molecule with an average lifetime τ, and another when after dissociation the velocity of separation of the fragments is sufficiently low that the molecule rotates during that dissociation [3]. Finally, there can be additional vibrational motion such that the orientation of the bond that is breaking has changed between excitation and dissociation [7].

Similar considerations apply to dissociative photoionization (DPI) processes, which can be used to study molecular-frame photoelectron angular distributions (MFPADs). A molecular photoionization experiment is said to be "complete" when it determines all the information needed for the theoretical description of such a process, which means to provide all the significant matrix elements or dynamical parameters [8]. There are different experimental methods for obtaining the matrix elements from the PADs for molecular ionization,

depending on the frame of reference used. When the measurement is done on a fixed-in-space molecule, it is referred to as the molecular frame photoelectron angular distribution (MFPAD) and, can be written as [9–14],

$$I(\theta_k, \phi_k, \theta_n, \phi_n) = \frac{4\pi^2}{c} E \sum_{L=0}^{\infty} \sum_{M=-L}^{L} \sum_{L'=0}^{2} \sum_{M'=-L'}^{L'} A_{LML'M'} Y_{LM}(\theta_k, \phi_k) Y_{L'M'}(\theta_n, \phi_n) \qquad (2)$$

where θ_n and ϕ_n are the polar and azimuthal angles for the direction of the polarization of the light, and θ_k and ϕ_k are the polar and azimuthal angles of the direction of emission of the photoelectron.

There are a number of methods that give information which can be related to the MFPADs [15]. One way of measuring the MFPAD is through DPI. If the dissociation event is rapid in comparison to the rotation period of the molecular ion and rapid compared to bending motions in the molecule then the ARA can be invoked so that the recoil directions of the fragments can be used to approximate the direction of the bonds that are being broken at the time of the initial ionization [2, 10, 16]. When the ARA is not valid, the photoelectron angular distributions can only be determined in the frame of reference provided by the direction of emission of the heavy fragments, referred to here as the recoil frame, leading to the recoil-frame photoelectron angular distribution (RFPAD). In the case of non-linear molecules, which are the subject of this work, even if the ARA is valid but only two fragments are produced in the DPI, there is necessarily an average over the azimuthal angle, which defines the orientation of the molecule about the recoil axis [10]. This leads to what we will refer to as the azimuthally-averaged RFPAD (AA-RFPAD). There have been several studies of the PADs from non-linear polyatomic molecules using dissociative photoionization where only two heavy fragments are produced so that the AA-RFPADs have been measured [10, 17–21]. However, in cases where the molecule breaks into three or more fragments it may be possible to determine the full RFPAD, where all three Euler angles defining the orientation of the recoil frame are measured. This full RFPAD is just the MFPAD when the ARA is valid [20, 22].

The effect of molecular rotation in slow dissociation processes has on observed RFPADs has been previously explored for the dissociation of the non-linear CF_3I molecule in the $\tilde{A}$ state of the ion. In that study a smearing of the PAD was found that could be explained by including rotation of the molecular frame after the electron ejection and before the fragmentation process [19]. This earlier work essentially used a linear model for the molecule

and a classical treatment of rotation which is valid for lifetimes that are less than the rotational period of the molecule.

In the present work, we develop expressions for the RFPADs that are similar to the ones published for linear molecules [10, 13, 23], which have been used to study a variety of linear systems' PADs in the molecular and recoil frames of reference [8, 12, 13, 24–30]. We include a fully quantal treatment of the three-dimensional rotational wave functions of non-linear molecules. These expressions will allow us to consider dissociative states with a wide range of lifetimes of the metastable molecular ions where the ARA cannot be used [12].

As a specific example of our general treatment of the effects of rotation in non-linear systems on PADs, we will consider the case of C $1s$ ionization of CH_4 where including the effects of rotation will be seen to improve the agreement between theory and experiment. We compare our results with experimental findings and with theory where the ARA has been assumed [20]. In addition to the effects of rotation studied here, the breakdown in the ARA can also be due to vibrational motion that occurs between the initial ionization and the subsequent fragmentation of the molecular ion. Thus our inferred lifetime of the ion state, when only rotation is included, will be an upper bound to the actual lifetime of the CH_4^{++} molecules produced by the Auger decay of the CH_4^+ core hole state.

Williams *et al.* [20] have studied the photoelectron angular distributions in C $1s$ photoionization of CH_4. They made coincidence measurements of the photoelectron with two and three heavy fragments. Assuming the ARA, the three-fragment measurements lead to experimental MFPADs. They also reported corresponding computed MFPADs and AA-RFPADs obtained using the complex Kohn method [20] and using the ARA approximation. The computed MFPADs were in quite reasonable agreement with the measured three-fragment MFPADs. However, the computed AA-RFPADs were only in agreement with the measured two-fragment AA-RFPADs when the kinetic energy release (KER) of the fragments was greater than 9 eV. Thus, there is clear evidence of the breakdown of the ARA in the fragmentation events leading to lower KERs.

II. RECOIL-FRAME PHOTOELECTRON ANGULAR DISTRIBUTIONS FOR ROTATING METASTABLE NON-LINEAR MOLECULAR IONS

The analysis of the RFPADs for non-linear polyatomic molecules follows closely the work that has been done previously for linear systems [9, 12]. Here we will consider RFPADs for light with general elliptical polarization as well as for the special cases of linearly and circularly polarized light. Throughout this derivation we have used different coordinate systems for convenience depending on the frame of reference used.

As mentioned above, if the lifetime of a molecular ion state represents a significant fraction of the rotational period of the molecule, then the ARA breaks down, and the effects of the rotational motion should be included when computing the cross sections. For this purpose, we assume a Boltzmann distribution of the rotational states [31], and follow a treatment that is similar to the one used for rotational motion in photodissociation by Jonah [6], assuming that the population of initial rotational states is thermal. After the molecule is ionized the density matrix elements for the rotational states are propagated in time. A Poisson distribution is assumed for the distribution of decay times.

A. Ionization of non-linear molecules and rotational state specific matrix elements

We consider the photoionization of non-linear molecules in the dipole approximation starting with the PAD in the field frame (FF) defined by the direction of propagation of the light and its polarization. The transition amplitude can be written as

$$T^{(\zeta',\zeta'')}_{\lambda,\delta}(\Omega_K,\hat{R}) = \sum_{l,m,n,\mu} \frac{1}{\sqrt{2}} \left\{ B_+ D^{(1)}_{\mu,-1}(\hat{R}) - B_- D^{(1)}_{\mu,1}(\hat{R}) \right\} I^{(\zeta',\zeta'')}_{lm\mu} Y^*_{ln}(\Omega_K) D^{(l)}_{m,n}(\hat{R}). \tag{3}$$

In this expression, the indices ζ' and ζ'' indicate a component of a degenerate set of initial and final states respectively, and λ and δ are the angles used to characterized the polarized light by the Stokes parameters (s_0, s_1, s_2, s_3) [32, 33] given by

$$s_0 = 1 \tag{4}$$

$$s_1 = \cos(2\lambda) \tag{5}$$

$$s_2 = \sin(2\lambda)\cos(\delta) \tag{6}$$

$$s_3 = \sin(2\lambda)\sin(\delta). \tag{7}$$

In the FF the direction of emission of the photoelectron is defined by the coordinates $\Omega_K = (\theta_K, \phi_K)$. The field is defined by B,

$$B = \frac{1}{\sqrt{2}} \left\{ B_+ \sum_{\mu=-1}^{1} e_\mu D^{(1)}_{\mu,-1}(\hat{R}) - B_- \sum_{\mu=-1}^{1} e_\mu D^{(1)}_{\mu,1}(\hat{R}) \right\} \tag{8}$$

and the D's are the usual rotational matrices defined elsewhere [34–36], $\hat{R}$ represents the Euler angles that describe the orientation of the field in the molecular frame (MF), the tensor operators e_μ are defined in the MF as

$$e_\mu = r Y_{1,\mu}(\theta, \phi) \sqrt{\frac{4\pi}{3}} = \begin{cases} z & \text{for } \mu = 0 \\ -\frac{x+iy}{\sqrt{2}} & \text{for } \mu = 1 \\ \frac{x-iy}{\sqrt{2}} & \text{for } \mu = -1 \end{cases}, \tag{9}$$

and $B_\pm$ is defined as

$$B_\pm = \cos\lambda \pm i \sin\lambda \exp(i\delta). \tag{10}$$

If the wave function for the continuum photoelectron, $\psi^{(-)}_{\Omega_k}(\vec{r})$, where the electron is emitted in the MF direction defined by $\Omega_k = (\theta_k, \phi_k)$, is expanded in partial waves $\psi^{(-)}_{lm}(\vec{r})$ as [37]

$$\psi^{(-)}_{\Omega_k}(\vec{r}) = \sqrt{\frac{2}{\pi}} \sum_{l,m} i^l \psi^{(-)}_{lm}(\vec{r}) Y^*_{lm}(\Omega_k), \tag{11}$$

then the partial-wave dipole matrix elements of Eq. (3) for photoionization going from an initial state $\Psi^{(\mathrm{i})}$ to a final state $\Phi^{(\mathrm{f})}$ are defined as

$$I^{(\zeta',\zeta'')}_{lm\mu} = \sqrt{\frac{2}{\pi}} i^l \left\langle \Psi^{(\mathrm{i})}_{\zeta'} \right| e_\mu \left| \Phi^{(\mathrm{f})}_{\zeta''} \psi^{(-)}_{lm}(\vec{r}) \right\rangle. \tag{12}$$

We express the asymmetric top rotational wave function, $\psi_{J,M_J,\kappa}$, as a linear combination of symmetric top wave functions $\phi_{J,M_J,H}$ [38],

$$\psi_{J,M_J,\kappa}(\hat{R}) = \sum_H C^{(J)}_{H,\kappa} \phi_{J,M_J,H}(\hat{R}) \tag{13}$$

where the symmetric top wave functions have the well known form,

$$\phi_{J,M_J,H}(\hat{R}) = \left(\frac{2J+1}{8\pi^2} \right)^{\frac{1}{2}} D^{(J)}_{-M_J,-H}(\hat{R}^{-1}), \tag{14}$$

where $\hat{R}^{-1}$ represents the Euler angles describing the orientation of the MF in the laboratory frame, *i.e.* in the FF. In this way, we construct the rotational state specific matrix elements

for the transitions $(\zeta, J, M_J, \kappa \leftarrow \zeta'', J'', M_{J''}, \kappa'')$ using the asymmetric top wave functions from Eq. (13) for the specific rotational states to get

$$T_{\lambda,\delta}^{(\zeta,J,M_J,\kappa\leftarrow\zeta'',J'',M_{J''},\kappa'')}(\Omega_K) = \int \left[\psi_{J'',M_{J''},\kappa''}(\hat{R})\right]^* \psi_{J,M_J,\kappa}(\hat{R}) T_{\lambda,\delta}^{(\zeta'',\zeta)}(\Omega_K,\hat{R}) d\hat{R} \tag{15}$$

where the substitution of Eq. (3) into Eq. (15) gives the full expression for the amplitude.

B. Thermal average and propagation in time

By assuming an equilibrium Boltzmann distribution of initial rotational states we can write the density matrix before the interaction with light, in analogy to the treatment of the rotational motion in photodissociation by Jonah [6], as

$$\rho = \frac{1}{g_{\rm i} Q(T)} \left\{ \sum_{\substack{\zeta'',J'' \\ M_{J''},\kappa''}} \left|\psi_{J'',M_{J''},\kappa''}\Psi_{\zeta''}^{(\rm i)}\right\rangle g_{\kappa''} \exp\left(-\frac{E_{J'',\kappa''}}{k_B T}\right) \left\langle \psi_{J'',M_{J''},\kappa''}\Psi_{\zeta''}^{(\rm i)}\right| \right\} \tag{16}$$

where $g_{\rm i}$ is the degeneracy of initial electronic states, $\Psi_{\zeta''}^{(\rm i)}$, $Q(T)$ is the rotational partition function for the initial state for an asymmetric-top molecule [39] and $g_{\kappa''}$ is the nuclear-spin statistical weight, which depends on the parities of the quantum numbers collectively labeled here as κ''.

After interaction with light, the density matrix propagated in time gives,

$$\rho''(t) = \frac{4\pi^2 E}{c} \exp\left(\frac{-iH_{\rm rot}t}{\hbar}\right) B^* \rho B \exp\left(\frac{iH_{\rm rot}t}{\hbar}\right) \tag{17}$$

where B is the field operator given in Eq. (8), E is the photon energy, and c is the speed of light. The density matrix given in Eq. (17) can be written in the coordinate representation by expanding ρ'' in final state functions, to give

$$\begin{aligned}\rho''(\Omega_{K'},\hat{R}',\Omega_K,\hat{R},t) = & \sum_{\substack{J,M_J,\kappa,\zeta \\ J',M_{J'},\kappa',\zeta'}} \left\langle \hat{R}'\right| \left.\psi_{J',M_{J'},\kappa'}\right\rangle \\ & \times \left\langle \psi_{J',M_{J'},\kappa'}\Phi_{\zeta'}^{(\rm f)}\psi_{\Omega_{K'}}^{(-)}\right| \rho''(t) \left|\psi_{J,M_J,\kappa}\Phi_{\zeta}^{(\rm f)}\psi_{\Omega_K}^{(-)}\right\rangle \left\langle \psi_{J,M_J,\kappa}\right| \left.\hat{R}\right\rangle . \end{aligned} \tag{18}$$

C. RFPADs for non-linear molecules including the effects of rotation

In the FF, the probability of detecting the photoelectron emitted in the direction Ω_K with the orientation of the molecule given by $\hat{R}^{-1}$ at time t, $I(\Omega_K,\hat{R},t)$, is given by the

diagonal elements of the density matrix given in Eq. (18), *i.e.*

$$I(\Omega_K, \hat{R}, t) = 8\pi^2 \rho''(\Omega_K, \hat{R}, \Omega_K, \hat{R}, t). \tag{19}$$

Finally, by assuming a Poisson distribution of decay times $(1/\tau)\exp(-t/\tau)$, the density matrix can be averaged over decay time to give

$$\begin{aligned} I_{\tau,T}(\Omega_k, \hat{R}) = & \frac{1}{g_{\rm i} Q(T)} \sum_{L',L,N,N'} Y_{L',-N'}(\Omega_k) E^{(\lambda,\delta)}_{L,N}(\hat{R}) \\ & \times \sum_{\substack{\zeta,\zeta'' \\ J,J',J'' \\ \kappa,\kappa',\kappa''}} g_{\kappa''} \exp\left(-\frac{E_{g_s,J'',\kappa''}}{k_B T}\right) \frac{H^{\binom{J,J',J''}{\kappa,\kappa',\kappa''}}_{L',N',L,N;(\zeta,\zeta'')}}{1 + \frac{i\tau \Delta E^{(J,\kappa,J',\kappa')}}{\hbar}} \end{aligned} \tag{20}$$

where again $\hat{R}$ gives the orientation of the field in the MF at the time of the decay and we have written the ejection direction of the photoelectron in the MF as Ω_k, and where

$$\begin{aligned} H^{\binom{J,J',J''}{\kappa,\kappa',\kappa''}}_{L',N',L,N;(\zeta,\zeta'')} = & \frac{4\pi^2 E}{c} \sum_{l,p,q,l'} \sum_{q''} (2J+1)(2J'+1)(2J''+1) \left[\frac{(2L'+1)(2l+1)}{(2l'+1)(2L+1)}\right]^{1/2} \\ & \times C^{J'}_{H'_2,\kappa'} C^{J*}_{H_1,\kappa} \times (-1)^{q-N+1} \langle L', N', l, -p |\, l', N'-p\rangle \\ & \times \langle L', 0, l, 0 |\, l', 0\rangle \langle 1, -q', 1, q |\, L, N\rangle \\ & \times M^{(J,J'',l,\kappa'',\zeta'',\zeta)}_{q'',p,q} \left[M^{(J',J'',l',\kappa'',\zeta'',\zeta)}_{q'',p',q'}\right]^*, \end{aligned} \tag{21}$$

where $\langle j_1, m_1, j_2, m_2 |\, J, M\rangle$ defines a Clebsch-Gordan coefficient, and $E^{(\lambda,\delta)}_{L,N}$ is defined in terms of the Stokes parameters as

$$\begin{aligned} E^{(\lambda,\delta)}_{L,N}(\hat{R}) = & \frac{1}{2}\sqrt{\frac{2L+1}{4\pi}} \Big\{ (1-s_3) \langle 1,1,1,-1 |\, L, 0\rangle D^{(L)}_{N,0}(\hat{R}) \\ & - (s_1 - i s_2) \langle 1,1,1,1 |\, L, 2\rangle D^{(L)}_{N,2}(\hat{R}) - (s_1 + i s_2) \langle 1,-1,1,-1 |\, L, -2\rangle D^{(L)}_{N,-2}(\hat{R}) \\ & + (1+s_3) \langle 1,-1,1,1 |\, L, 0\rangle D^{(L)}_{N,0}(\hat{R}) \Big\}, \end{aligned} \tag{22}$$

and where

$$\begin{aligned} M^{(J,J'',l,\kappa'',\zeta'',\zeta)}_{q'',p,q} = & \sum_{m,\mu} I^{(\zeta'',\zeta)}_{lm\mu} \sum_K (-1)^{\kappa''-q''+m+p} \left[\frac{2K+1}{3(2J+1)}\right] \\ & \langle K, m+\mu, J'', -\kappa'' |\, J, m+\mu-\kappa''\rangle \\ & \times \langle K, q+p, J'', q'' |\, J, q+p+q''\rangle \langle K, \mu+m, l, -m |\, 1, \mu\rangle \\ & \times \langle K, q+p, l, -p |\, 1, q\rangle . \end{aligned} \tag{23}$$

By defining $H^{(\tau,T)}_{L',N',L,N}$ as

$$H^{(\tau,T)}_{L',N',L,N} = \frac{1}{g_i Q(T)} \sum_{\substack{\zeta,\zeta'' \\ J,J',J'' \\ \kappa,\kappa',\kappa''}} g_{\kappa''} \exp\left(-\frac{E_{g_s,J'',\kappa''}}{k_B T}\right) \frac{H^{\binom{J,J',J''}{\kappa,\kappa',\kappa''}}_{L',N',L,N;(\zeta,\zeta'')}}{1+\frac{i\tau\Delta E^{(J,\kappa,J',\kappa')}}{\hbar}} \tag{24}$$

we can write the intensity as

$$I^{(\lambda,\delta)}_{\tau,T}(\Omega_k,\hat{R}) = \sum_{L',L,N,N'} Y_{L',-N'}(\Omega_k) E^{(\lambda,\delta)}_{L,N}(\hat{R}) H^{(\tau,T)}_{L',N',L,N}. \tag{25}$$

Lastly, for the special cases of polarization where the parameter μ_0 is defined such that $\mu_0 = 0$ for linearly polarized light with $\lambda = 0$, $\mu_0 = +1$ for left-circularly polarized light with positive helicity with $\lambda = \frac{\pi}{4}$ and $\delta = \frac{-\pi}{2}$, and $\mu_0 = -1$ for right-circularly polarized light with negative helicity with $\lambda = \frac{\pi}{4}$ and $\delta = \frac{\pi}{2}$, Eq. (25) for the intensity becomes [40]

$$I^{(\mu_0)}_{\tau,T}(\Omega_k,\Omega_n) = \sum_{L,N,L',N'} (-1)^{\mu_0+1} \langle 1,-\mu_0,1,\mu_0|\ L,0\rangle\ H^{(\tau,T)}_{L',N',L,N} Y_{L',-N'}(\Omega_k) Y^*_{LN}(\Omega_n) \tag{26}$$

where for linearly polarized light Ω_n is the direction of polarization and for circularly polarized light Ω_n is the direction of propagation of the light, both in the MF.

To compute the AA-RFPADs, it is necessary to include an average of the full RFPADs over the azimuthal angle about the recoil direction, and after this average we obtain the expression [21],

$$I^{(\mathrm{ion})}_{\mu_0,\beta_\mathrm{R},\alpha_\mathrm{R}}(\Omega_k,\Omega_n) = \sum_{L',L,Q} H^{\mu_0,\beta_\mathrm{R},\alpha_\mathrm{R}}_{L',L,Q} Y_{L',Q}(\Omega_k) Y^*_{L,Q}(\Omega_n) \tag{27}$$

where the angles β_R and α_R define the recoil direction in the molecular frame and the direction of the field and photoelectron momentum in the recoil frame are given by Ω_n and Ω_k, respectively. The coefficients $H^{\mu_0,\beta_\mathrm{R},\alpha_\mathrm{R}}_{L',L,Q}$ are given by

$$\begin{aligned} H^{\mu_0,\beta_\mathrm{R},\alpha_\mathrm{R}}_{L',L,Q} = \sum_{J,N',N,P} H^{(\tau,T)}_{L',N',L,N} \left[\frac{4\pi(2J+1)}{(2L'+1)^2}\right]^{1/2} (-1)^{\mu_0+1} \langle 1,-\mu_0,1,\mu_0|\ L,0\rangle \\ \times \langle J,0,L,Q|\ L',Q\rangle \langle J,P,L,N|\ L',-N'\rangle\, Y_{J,P}(\beta_\mathrm{R},\alpha_\mathrm{R}) \end{aligned} \tag{28}$$

where $P = -(N'+N)$ and $H^{(\tau,T)}_{L',N',L,N}$ is given in Eq. (24).

III. EFFECTS OF ROTATIONAL MOTION ON THE C 1s PHOTOIONIZATION OF CH_4

A. Computation of the photoionization dipole matrix elements

The dynamical photoionization matrix elements, $I_{lm\mu}^{(\zeta',\zeta'')}$, from Eq. (3) leading to the C 1s $(1a_1)^{-1}$ state of CH_4 were computed using the Schwinger variational method [41, 42]. An $l_{\max} = 100$ was used for the single-center expansion of the electronic wave functions within the single-channel frozen-core Hartree-Fock approximation (SCFCHF) using the ePolyScat suite of programs [43, 44], within the fixed-nuclei approximation. The initial and final bound electronic state wave functions, $\Psi_{\rm i}(r,q)$ and $\Psi_{{\rm f},\vec{k}}^{(-)}(r,q)$ were calculated at the Hartree-Fock level of theory using the augmented correlation-consistent polarized valence triple-ζ [45, 46] (aug-cc-pVTZ) basis set and were computed using the Gaussian09 program [47]. For these calculations a vertical ionization potential (ionization from the C 1s) of 290.84 eV [48] and a bond length of 1.087 Å[49] were used. The rotational constant used was 5.2891694 cm $^{-1}$ and was computed using the fixed geometry within the rigid rotor model.

B. MFPADs and full RFPADs for CH_4

We first examine the MFPADs and full RFPADs for the CH_4 C 1s photoionization. The methane molecule, shown in Fig. 1, has tetrahedral symmetry, belonging to the T_d point group, and therefore it has four equivalent C_3 axes of symmetry and three equivalent C_2 axes. Each of the CH bonds lies on a C_3 axis. In Figs. 2 through 4 the molecule is oriented so that one of the C_2 symmetry axes coincides with the z cartesian axis, as shown in Fig. 1. The ground state electronic configuration of CH_4 is $(1a_1)^2(2a_1)^2(1t_2)^6$, where the $1a_1$ orbital is essentially the atomic 1s orbital on the central carbon atom.

The MFPADs and full RFPADs for the ionization from the $1a_1$ orbital were computed at photoelectron energies $E_k = 0.1, 4.35$ and 15.25 eV as described above. These photoelectron kinetic energies are represented in that order in Figs. 2 to 4 for ionization with linearly polarized light (LP), that is $\mu_0 = 0$. As it was pointed out by Lucchese [9], the shape of the MFPADs can be understood, at least qualitatively, by considering the angular momentum composition of the initial orbitals and the angular momentum contribution from the different polarizations of the ionizing light. For the case analyzed here, ionization from an s orbital,

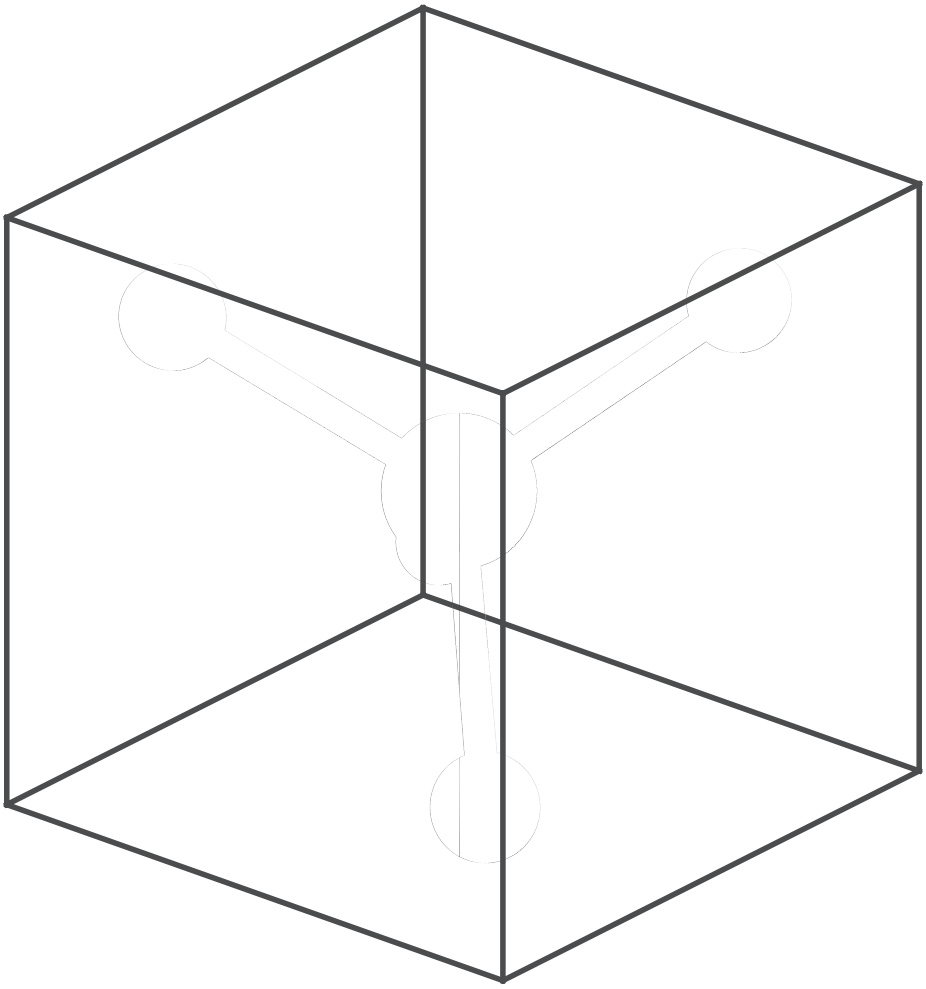

FIG. 1. Schematic representation of the methane molecule as oriented in the calculations.

in the absence of scattering, the photoelectron leaves in a p wave and the orientation of the MFPAD is determined by the orientation of the polarized light. If we look at the first row of Fig. 2, where the lifetime of the pre-dissociative state is assumed to be $\tau = 0$ ps, implying the validity of the ARA, the MFPADs look different from what is expected from simple angular momentum considerations discussed above due to the effects of scattering of the photoelectron by a non-spherical field. The corresponding full RFPADs obtained assuming non-zero predissociative lifetimes, τ, from 0.16 ps to infinite lifetime are given in subsequent rows of Fig. 2. As the lifetimes increase, the shape of the full RFPADs approaches the result given in Eq. (1) with $\beta = 2$, as would be expected for ionization from an s state. Williams *et al.* [20] report computed MFPADs obtained using the complex Kohn method within the ARA approximation that are in very good agreement with their measured MFPADs. The

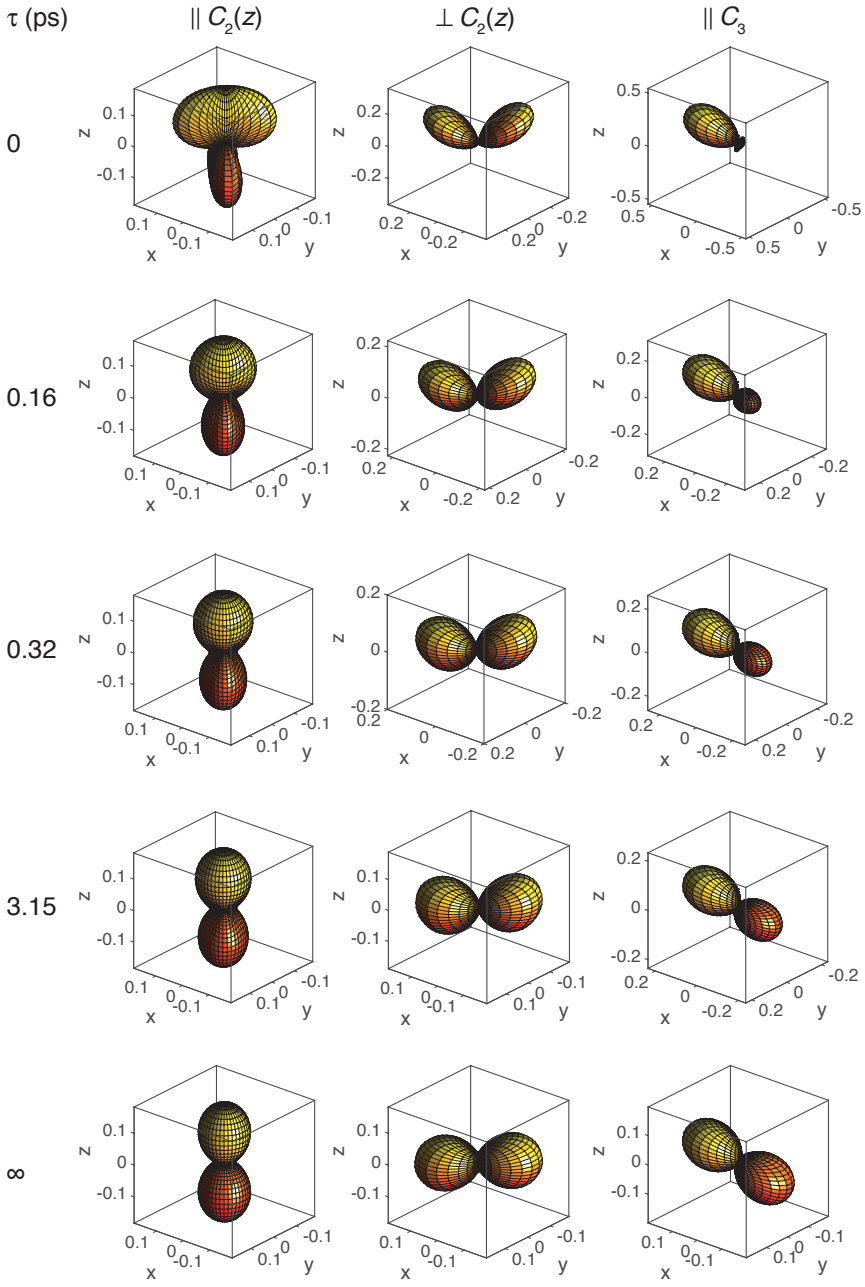

FIG. 2. MFPADs and full RFPADs for the photoionization of the C 1s orbital of CH_4 molecule. Results computed at $E_k = 0.1$ eV for linearly polarized light (LP). In each column the polarization vectors change: first parallel to the C_2 axis in the z direction; second, perpendicular to the $C_2(z)$ axis and in the plane with two CH bonds; and third, parallel to a C_3 axis (CH bond). Lifetimes of the pre-dissociative state are indicated for each row. The axes are in units of MBarn/sr. The molecular orientation is shown in Fig. 1.

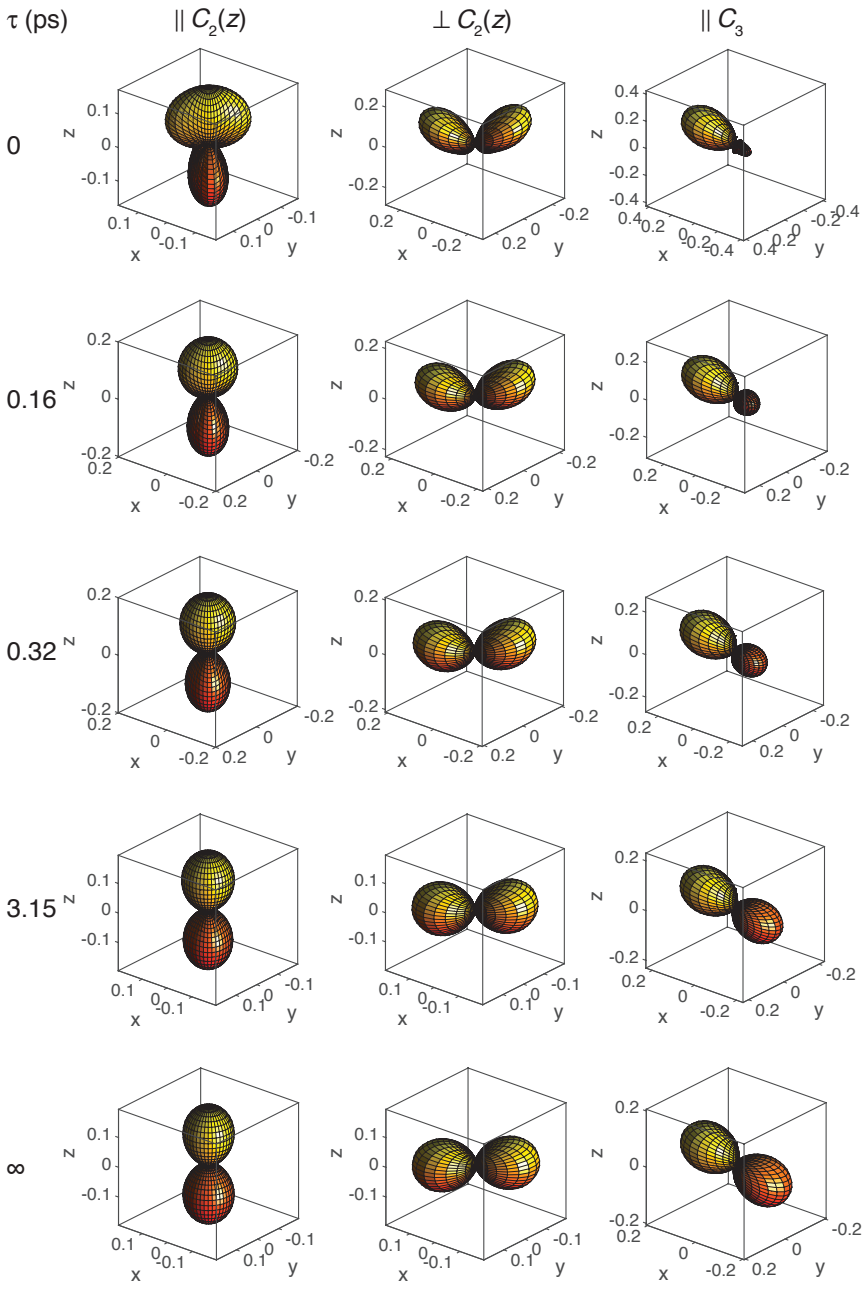

FIG. 3. MFPADs and full RFPADs for the photoionization of the C 1s orbital of CH_4 molecule. Results computed at $E_k = 4.35$ eV for linearly polarized light (LP). In each column the polarization vectors change: first parallel to the C_2 axis in the z direction; second, perpendicular to the $C_2(z)$ axis and in the plane with two CH bonds; and third, parallel to a C_3 axis (CH bond). Lifetimes of the pre-dissociative state are indicated for each row. The axes are in units of MBarn/sr. The molecular orientation is shown in Fig. 1.

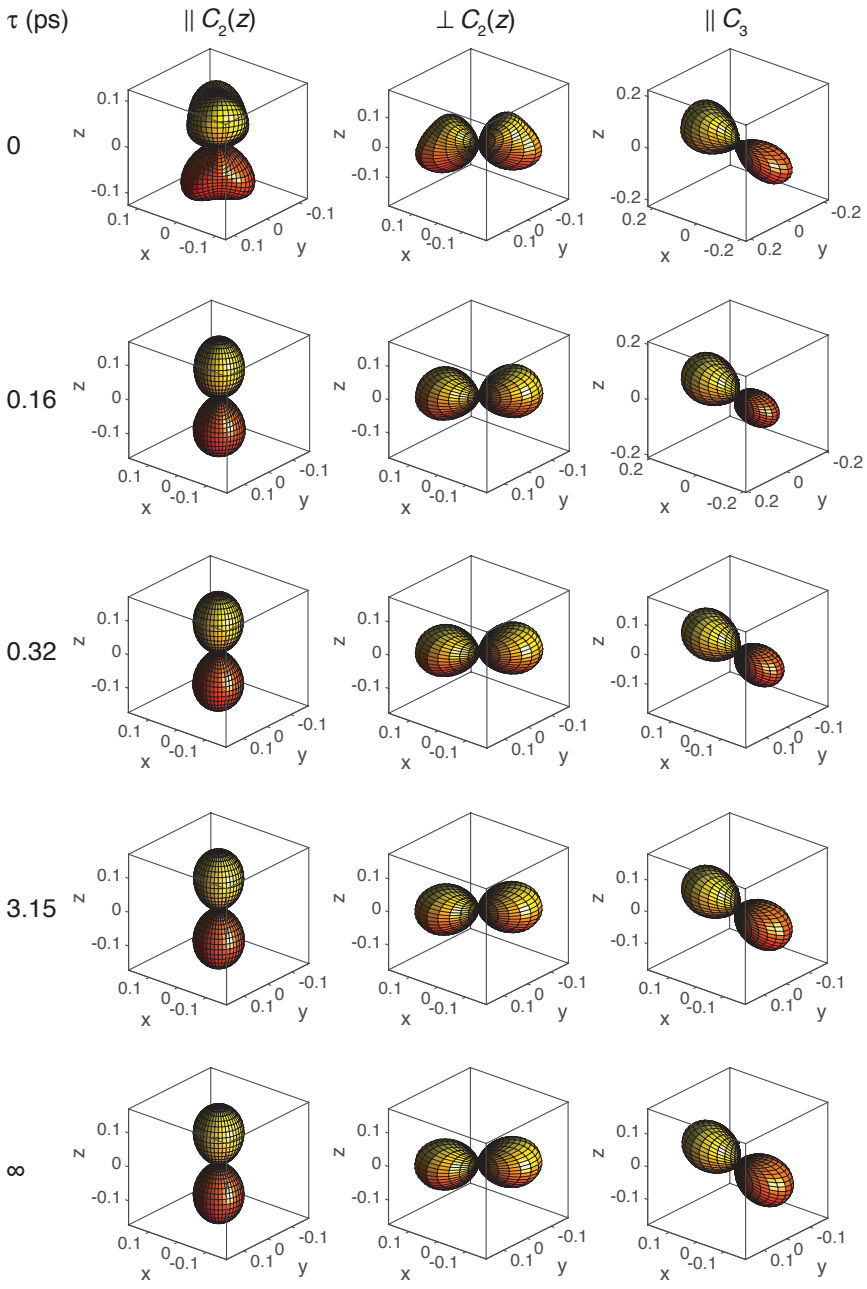

FIG. 4. MFPADs and full RFPADs for the photoionization of the C 1s orbital of CH_4 molecule. Results computed at $E_k = 15.25$ eV for linearly polarized light (LP). In each column the polarization vectors change: first parallel to the C_2 axis in the z direction; second, perpendicular to the $C_2(z)$ axis and in the plane with two CH bonds; and third, parallel to a C_3 axis (CH bond). Lifetimes of the pre-dissociative state are indicated for each row. The axes are in units of MBarn/sr. The molecular orientation is shown in Fig. 1.

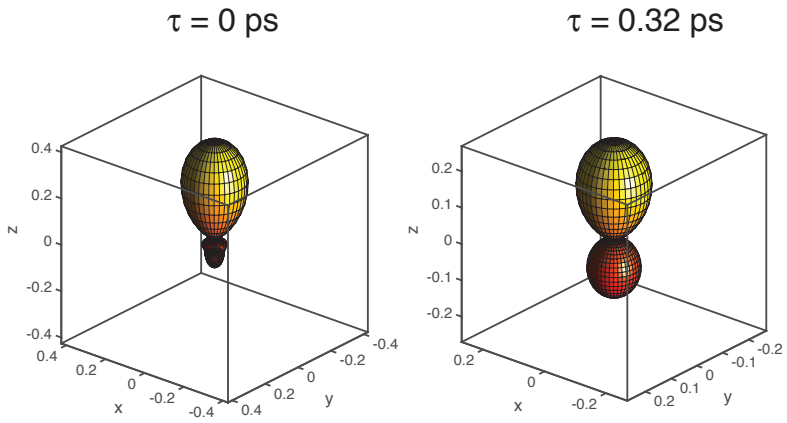

FIG. 5. Two-fragment RFPADs for the photoionization from the C 1s orbital of CH_4 molecule. Results computed at $E_k = 4.35$ eV for linearly polarized light (LP). The orientation average was performed around a CH bond, that is a C_3 axis, in this plot pointing in the z direction, and the orientation of the polarization of the LP light is also aligned with the C_3 axis in this figures. The figure at the left assumes a lifetime of the state of 0 ps, and the figure at the right of 0.32 ps. The axes are in units of MBarn/sr.

MFPADs computed here with $\tau = 0$ are very similar to the previously published results.

C. Azimuthally-averaged RFPADs for CH_4

Two-heavy-fragment coincidences, e^-+ H^++ CH_3^+, were measured by Williams *et al.* [20] and the resulting AA-RFPADs were found to depend on the fragment kinetic energy release (KER) in the fragments. High KER leads to AA-RFPADs consistent with the ARA. However, low KER events indicate a breakdown in the ARA suggesting that the different KERs correspond to different pathways, *e.g.* different CH_4^{++} states populated by Auger decay. We show here that a non-zero predissociation lifetime can reproduce measured AA-RFPADs. These lifetimes are the upper limits to the true lifetimes where other vibrational dynamics could explain some of the deviation from the ARA and thus shortening the dissociative lifetime needed to obtain agreement between theory and experiment.

In Fig. 5 we present the AA-RFPADs for the C 1s photoionization of methane at a photoelectron energy $E_k = 4.35$ eV, with the vector of polarization of the light in the

direction of one of the CH bonds, and orientation averaged about that same axis, which in the figures appears pointing in the z direction. In the experimental data [20], the observed AA-RFPADs depended on the KER. With a lifetime of $\tau = 0$ ps our computed AA-RFPAD is obtained within the ARA, *i.e.* not including rotation, with the recoil axis in the direction of the CH bond. These results agree with the previous computed AA-RFPADs [20], which were also obtained using the ARA, and with the experimental data for KER > 9 eV. As the assumed lifetime of the pre-disociative state is increased to $\tau = 0.32$ ps, allowing for the molecular ion before fragmentation, the AA-RFPAD exhibits a breakdown of the ARA and shows a better agreement with the experiments [20] when lower KER (< 7 eV) are considered.

In Fig. 6 we can compare the AA-RFPADs for different measured KERs [20] and the computed AA-RFPADs from this work. We can see a very good agreement between theory and experiment when we assign different lifetimes for the pre-dissociative state and compare them to the RFPADs as a function of $\cos(\theta)$ for different KERs. In Fig. 7 it is very clear that the photoelectron angular distributions of this DPI process indicate there is a breakdown of the ARA. For KER > 9 eV, assuming an almost instantaneous dissociation, close to the ARA, with a lifetime of $t = 0.05$ ps gives a very good agreement with the experiments, similar to the theoretical study presented in reference [20]. However when the ARA is not valid, as shown in the right panel of Fig. 7, for low kinetic energy fragments, KER < 7 eV, using the rotation of the molecule as the mechanism for the breakdown of the ARA a rotational lifetime on the order of 0.5 ps or longer of the pre-dissociative state leads to good agreement between the experimentally observed and our computed AA-RFPADs.

The fragmentation of the molecule, observed in the experiment, occurs on a double ion potential surface after the Auger decay of the initially formed C $(1s)^{-1}$ hole state of CH_4. The width of the hole state has been measured as 83 ± 10 meV [50] with a corresponding lifetime of 7.9 fs. Thus the only possible source of a long lifetime before dissociation would be the dynamics of the double ion. In addition to rotation, the breakdown of the ARA could also be due to bending motions in the double ion before fragmentation. The good agreement between the present theory and the observed RFPADs sets an upper bound on the lifetime of the double-ion states and would indicate that the the measured RFPADs cannot by themselves distinguish between vibrational dynamics or rotational motion as the source of the breakdown of the ARA.

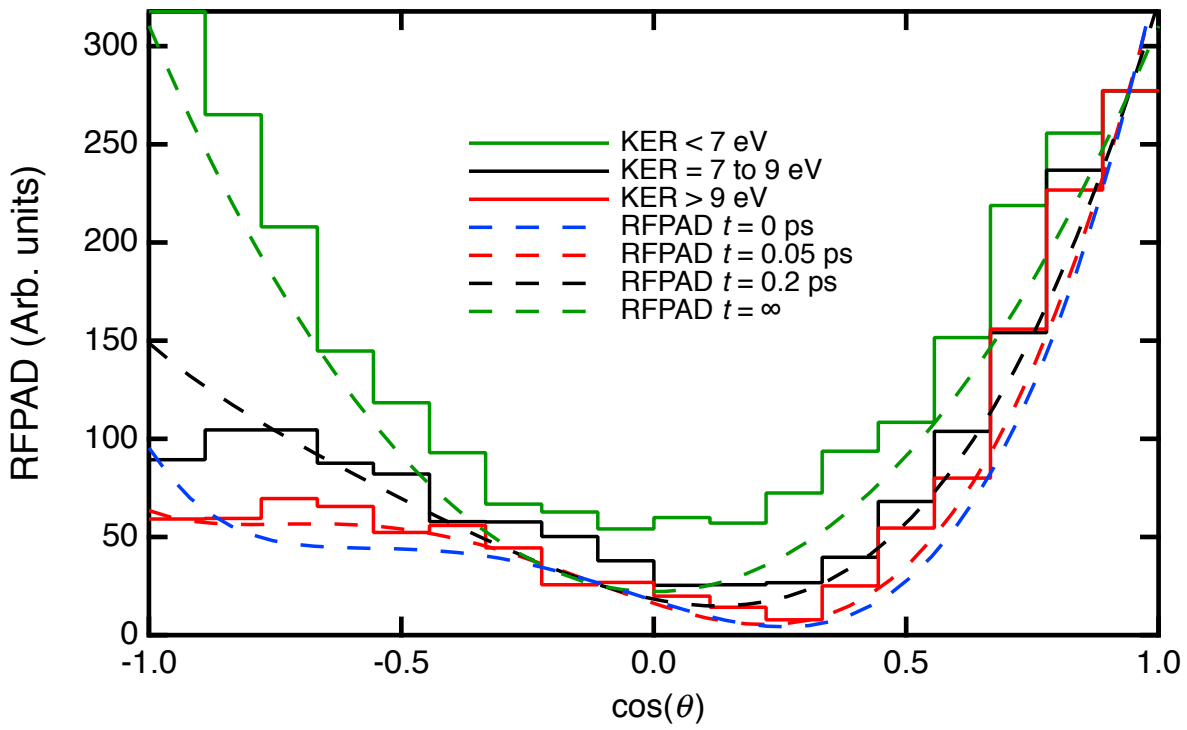

FIG. 6. Two-fragment RFPADs as a function of $\cos(\theta)$. Experimental measurements from reference [20] in solid lines exhibit the distributions for different KER fragments and the theoretical results from this work in dashed lines show the distributions for fragments with different lifetimes as indicated within the figure.

IV. CONCLUSIONS

We presented a theoretical model for computing MFPADs and RFPADs for non-linear molecules that includes the effect of rotational motion between ionization and fragmentation. This model can be used to predict RFPADs for systems where the axial-recoil approximation breaks down. The predicted MFPADs for the C $(1s)^{-1}$ photoionization of methane were in good agreement with previous theoretical predictions [20] within the ARA, *i.e.* with no rotation. Our computed RFPADs exhibit good agreement with the low KER experiments when we treat the breakdown of the ARA as rotation before dissociation with a delay time of 0.5 ps, which is a considerable fraction of the rotational period of CH_4 which is 3 ps. Although our rotation model gives very good agreement with the experimental data, one cannot exclude the possibility that the same RFPADs could be obtained by vibrational

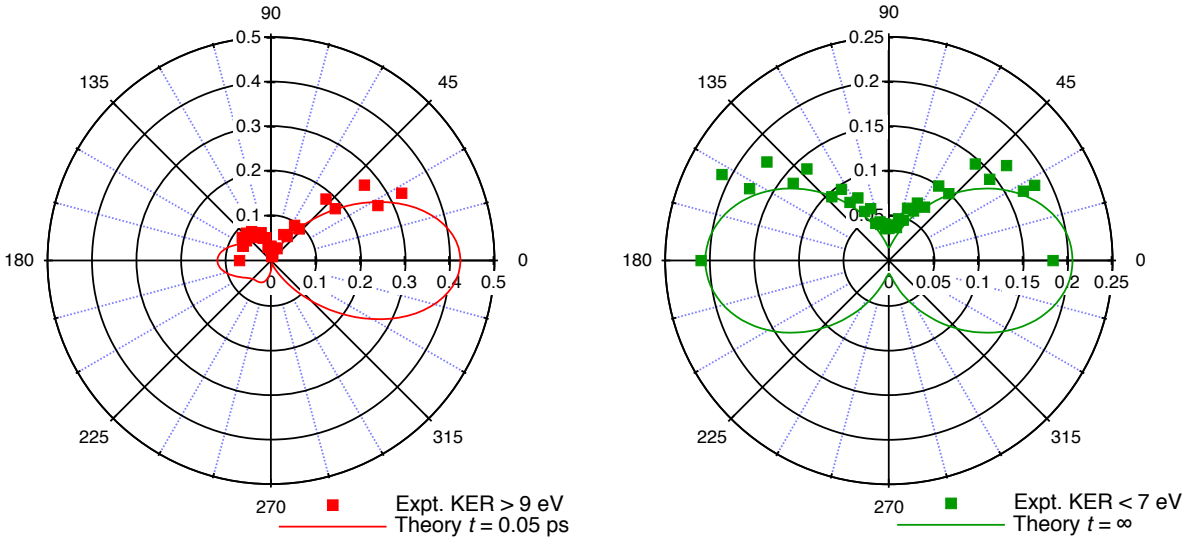

FIG. 7. Polar plots of the theoretical (solid lines) and experimental (squares) two-fragment RF-PADs for photoelectron kinetic energy of $E_k = 4.35$ eV. At the left, in red, experimental data shows the distribution of fragments with KER > 9 eV and theoretical distributions for fragments with lifetime $t = 0.05$ ps. At the right, in green, experimental data shows the distribution of fragments with KER < 7 eV and theoretical distributions for fragments with infinite lifetime t. The experimental data, taken from reference [20], is not absolute, and here has been scaled for the best agreement with the computed data. The axes are in units of MBarn/sr.

motion of the CH_4^{++} before dissociation. This model extends the possibilities of studying dynamics of photoionization of valence states of polyatomic molecules using angle-resolved photoelectron-photoion coincidence measurements where the ARA is often not a good approximation [21].

V. ACKNOWLEDGMENTS

We gratefully acknowledge support of this work by the United States Department of Energy, Office of Science, Basic Energy Science, Geoscience, and Biological Divisions under Award No. DE-SC0012198. JAL was partially supported by the Robert A. Welch Foundation (Houston, TX) under Grant No. A-1020. Also the assistance and computer time provided by the Supercomputing Facility at Texas A&M University is acknowledged. Help-

ful discussions with C. W. McCurdy about these results are also gratefully acknowledged.

---

[1] T. P.Rakitzis, and R. N. Zare, *J. Chem. Phys.* **110**, 3341 (1999).

[2] R. N. Zare, *Mol. Photochem.* **4**, 1 (1972).

[3] S.-C. Yang, and R. Bersohn, *J. Chem. Phys.* **61**, 4400 (1974).

[4] R. N. Zare and D. R. Herschbach, *Proc. IEEE* **51**, 173 (1963).

[5] R. Bersohn and S. H. Lin, *Adv. Chem. Phys.* **16**, 67 (1969).

[6] C. Jonah, *J. Chem. Phys.* **55**, 1915 (1971).

[7] T. P. Rakitzis, A. J. van den Brom, and M. H. M. Janssen, *Chem. Phys. Lett.* **372**, 187 (2003).

[8] M. Lebech, J. C. Houver, A. Lafosse, D. Dowek, C. Alcaraz, L. Nahon, and R. R. Lucchese, *J. Chem. Phys.* **118**, 9653 (2003).

[9] R. R. Lucchese, *J. Electron Spectrosc. Relat. Phenom.* **141**, 201 (2004).

[10] R. R. Lucchese, R. Carey, C. Elkharrat, J. C. Houver, and D. Dowek, *J. Phys. Conf. Ser.* **141**, 012009 (2008).

[11] K. L. Reid, *Annu. Rev. Phys. Chem.* **54**, 397 (2003).

[12] A. Lafosse, J. C. Brenot, P.M. Guyon, J. C. Houver, A. V. Golovin, M. Lebech, D. Dowek, P. Lin, and R. R. Lucchese, *J. Chem. Phys.* **117**, 8368 (2002).

[13] R. R. Lucchese, A. Lafosse, J. C. Brenot, P. M. Guyon, J. C. Houver, M. Lebech, G. Raseev, and D. Dowek, *Phys. Rev. A* **65**, 020702 (2002).

[14] D. Dill, *J. Chem. Phys.* **65**, 1130 (1976).

[15] R. R. Lucchese and D. Dowek, in *Attosecond and XUV Spectroscopy: ultrafast dynamics and spectroscopy*, edited by M. J. J. Vrakking and T. Schultz (Wiley, Hoboken, NJ, 2014), p. 293.

[16] R. N. Zare, *J. Chem. Phys.* **47**, 204 (1967).

[17] Y. Hikosaka, J. H. D. Eland, T. M. Watson, and I. Powis, *J. Chem. Phys.* **115**, 4593 (2001).

[18] P. Downie and I. Powis, *Phys. Rev. Lett.* **82**, 2864 (1999).

[19] P. Downie and I. Powis, *Faraday Discuss.* **115**, 103 (2000).

[20] J. B. Williams, C. S. Trevisan, M. S. Schöffler, T. Jahnke, I. Bocharova, H. Kim, B. Ulrich, R. Wallauer, F. Sturm, T. N. Rescigno, A. Belkacem, R. Dörner, Th. Weber, C. W. McCurdy, and A. L. Landers, *J. Phys. B: At. Mol. Opt.* **45**, 194003 (2012).

[21] D. Toffoli, R. R. Lucchese, M. Lebech, J. C. Houver, and D. Dowek, *J. Chem. Phys.* **126**, 054307 (2007).

[22] M. Yamazaki, J.-I. Adachi, T. Teramoto, A. Yagishita, M. Stener and P. Decleva, *J. Phys. B: At. Mol. Opt. Phys.* **42**, 051001 (2009).

[23] M. Lebech, J. C. Houver, D. Dowek, and R. R. Lucchese, *J. Chem. Phys.* **120**, 8226 (2004).

[24] P. Lin and R. R. Lucchese, *J. Chem. Phys.* **116**, 8863 (2002).

[25] A. Lafosse, M. Lebech, J. C. Brenot, P. M. Guyon, O. Jagutzki, L. Spielberger, M. Vervloet, J. C. Houver, and D. Dowek, *Phys. Rev. Lett.* **84**, 5987 (2000).

[26] J. H. D. Eland, M. Takahashi, and Y. Hikosaka, *Faraday Discuss.* **115**, 119 (2000).

[27] A. Lafosse, J. C. Brenot, A. V. Golovin, P. M. Guyon, K. Hoejrup, J. C. Houver, M. Lebech, and D. Dowek, *J. Chem. Phys.* **114**, 6605 (2001).

[28] A. V. Golovin, N. A. Cherepkov, and V. V. Kuznetsov, *Z. Phys. D At. Mol. Cl.* **24**, 371 (1992).

[29] T. Jahnke, Th. Weber, A. L. Landers, A. Knapp, S. Schössler, J. Nickles, S. Kammer, O. Jagutzki, L. Schmidt, A. Czasch, T. Osipov, E. Arenholz, A. T. Young, R. Díez Muiño, D. Rolles, F. J. García de Abajo, C. S. Fadley, M. A. Van Hove, S. K. Semenov, N. A. Cherepkov, J. Rösch, M. H. Prior, H. Schmidt-Böcking, C. L. Cocke, and R. Dörner, *Phys. Rev. Lett.* **88**, 073002 (2002).

[30] H. Fukuzawa, X-J. Liu, R. Montuoro, R. R. Lucchese, Y. Morishita, G. Prümper, and K. Ueda, *J. Phys. B At. Mol. Opt.* **41**, 045102 (2008).

[31] I. Levine, *Molecular spectroscopy*. Wiley, New York, N.Y., 1975.

[32] W. H. McMaster, *Am. J. Phys.* **22**, 351 (1954).

[33] R. G. Newton, *Scattering theory of waves and particles*. Dover Publications, 2nd edition, 2013.

[34] R. Zare, *Angular momentum: understanding spatial aspects in chemistry and physics*. Wiley Interscience, New York, N.Y., 1988.

[35] A. Edmonds, *Angular momentum in quantum mechanics*. Princeton University Press, Princeton, N.J., 1957.

[36] M. E. Rose, *Elementary theory of angular momentum*. Dover Publications, New York, N.Y., 1995.

[37] R. R. Lucchese, G. Raseev, and V. McKoy, *Phys. Rev. A* **25**, 2572 (1982).

[38] P. R. Bunker and P. Jensen, *Molecular symmetry and spectroscopy*. NRC Publications, 1998.

[39] J. K. G. Watson, *Mol. Phys.* **65**, 1377 (1988).

[40] J. A. López-Domínguez, Ph.D. Thesis, Texas A&M University, 2015.

[41] R. R. Lucchese and V. McKoy, *Phys. Rev. A* **21**, 112 (1980).

[42] R. E. Stratmann and R. R. Lucchese, *J. Chem. Phys.* **102**, 8493 (1995).

[43] A. P. P. Natalense and R. R. Lucchese, *J. Chem. Phys.* **111**, 5344 (1999).

[44] F. A. Gianturco, R. R. Lucchese, and N. Sanna, *J. Chem. Phys.* **100**, 6464 (1994).

[45] T. H. Dunning, *J. Chem. Phys.* **90**, 1007 (1989).

[46] R. A. Kendall, T. H. Dunning, and R. J. Harrison, *J. Chem. Phys.* **96**, 6796 (1992).

[47] M. J. Frisch, G. W. Trucks, H. B. Schlegel *et al.*, GAUSSIAN 09, (2009).

[48] V. Myrseth, J. D. Bozek, E. Kukk, L. J. Sæthre, and T. D. Thomas, *J. Electron Spectrosc. Relat. Phenom.* **122**, 57 (2002).

[49] E. Hirota, *J. Mol. Spectrosc.* **77**, 213 (1979).

[50] H. M. Köppe, B. S. Itchkawitz, A. L. D. Kilcoyne, J. Feldhaus, B. Kempgens, A. Kivimäki, M. Neeb, and A. M. Bradshaw, *Phys. Rev. A* **53**, 4120 (1996).